Upregulation of Bone Morphogenetic Protein-1/Mammalian Tolloid and Procollagen C-Proteinase Enhancer-1 in Corneal Scarring

François Malecaze, Dawiyat Massoudi, Pierre Fournié, Cyrielle Tricoire, Myriam Cassagne, Marilyne Malbouyres, David J. S. Hulmes, Catherine Moali, Stéphane Galiacy

Upregulation of Bone Morphogenetic Protein-1/ Mammalian Tolloid and Procollagen C-Proteinase Enhancer-1 in Corneal Scarring

Francois Malecaze,[1,2] Dawiyat Massoudi,[1] Pierre Fournié,[1,2] Cyrielle Tricoire,[1] Myriam Cassagne,[1,2] Marilyne Malbouyres,[3] David J. S. Hulmes,[4] Catherine Moali,[4] and Stephane D. Galiacy[1,2]

[1]Equipe d'Accueil (EA) 4555, Université Toulouse III Paul Sabatier, Toulouse, France
[2]Centre Hospitalier Universitaire (CHU) Toulouse, Hôpital Purpan, Service d'Ophtalmologie, Toulouse, France
[3]Unité Mixte de Recherche (UMR) 5242 Centre National de la Recherche Scientifique (CNRS)/Ecole Normale Supérieure de Lyon/ Université Lyon 1, Lyon, France
[4]UMR 5305 CNRS/Université Lyon 1, Lyon, France

Correspondence: Catherine Moali, Institut de Biologie et Chimie des Protéines, 7 passage du Vercors, 69367 Lyon, France; c.moali@ibcp.fr.
Stéphane D. Galiacy, EA 4555, Université Paul Sabatier, Hôpital Purpan, BP 3028, Place du Dr Baylac, 31024 Toulouse Cedex 3, France; sgaliacy@yahoo.fr.

FM and DM contributed equally to the work presented here and should therefore be regarded as equivalent authors.

Submitted: December 19, 2013
Accepted: September 4, 2014

Citation: Malecaze F, Massoudi D, Fournié P, et al. Upregulation of bone morphogenetic protein-1/mammalian tolloid and procollagen C-proteinase enhancer-1 in corneal scarring. *Invest Ophthalmol Vis Sci*. 2014;55:6712–6721. DOI:10.1167/iovs.13-13800

Purpose. To characterize the expression of the bone morphogenetic protein-1 (BMP-1)/tolloid-like proteinases (collectively called BTPs), which include BMP-1, mammalian tolloid (mTLD), and mammalian tolloid-like 1 (mTLL-1) and 2 (mTLL-2), as well as the associated proteins procollagen C-proteinase enhancers (PCPE-1 and -2), in corneal scarring.

Methods. Using a mouse full-thickness corneal excision model, wound healing was followed for up to 28 days by transmission electron microscopy, immunohistology (BMP-1/mTLD and PCPE-1), and quantitative PCR (Q-PCR: collagen III, BMP-1/mTLD, mTLL-1, mTLL-2, PCPE-1, PCPE-2). Bone morphogenetic protein-1/mTLD and PCPE-1 were also immunolocalized in cases of human corneal scarring following injuries.

Results. In the mouse model, throughout the follow-up period, there was a large increase in collagen III mRNA expression in the stroma. By transmission electron microscopy, there was marked cellular infiltration into the wound as well as disorganization of collagen fibrils, but no significant difference in fibril diameter. In control corneas, by Q-PCR, BMP-1/mTLD showed the highest expression, compared to low levels of mTLL-1 and undetectable levels of mTLL-2, in both epithelium and stroma. Following wounding, both BMP-1/mTLD and PCPE-1 mRNA and protein increased, while PCPE-2 mRNA decreased. Finally, by immunofluorescence, BMP-1/mTLD and PCPE-1 were strongly expressed in the scar region in both mouse and human corneas.

Conclusions. Bone morphogenetic protein-1/mTLD and PCPE-1 are upregulated in corneal scars. Both proteins may therefore contribute to the process of corneal scarring.

Keywords: BMP1, PCPE1, corneal wound healing, collagen

Corneal scars are associated with a loss of visual acuity and with blindness in the most severe cases. Corneal scarring is the major complication of refractive surgery and has become an important concern in ophthalmology.[1–5] Such scarring results from poor wound healing following surgery but also from other forms of trauma or infections. Due to the difficulties in anticipating and treating corneal scar, corneal transplantation remains the most efficient treatment available so far but also suffers from major drawbacks (lack of donors, graft rejection).

Corneal wound healing is a complex process orchestrated mainly by growth factors, cytokines, and extracellular proteases. Among growth factors, IL-1α, TGF-β2, and platelet-derived growth factor (PDGF) have been assigned important roles and, in the case of basement membrane disruption, can diffuse from their site of production, in the epithelial layer, toward the stroma.[6] However, persistent epithelial–stromal interactions are known to have deleterious effects on the healing process and are often responsible for the observed failures of photorefractive keratectomy (PRK).

Extracellular proteases have also been implicated in wound healing, where they can play various roles, ranging from synthesis/degradation of extracellular matrix proteins and activation/inactivation of cytokines and growth factors to the modulation of cell–matrix interactions and cell phenotype.[7] During the healing response, these proteases are provided by the tear fluid, sparse inflammatory cells invading the cornea from the surrounding limbus, injured epithelial cells, and stromal cells, which, depending on their state of activation, are called keratocytes, fibroblasts, or myofibroblasts. While matrix metalloproteinases (MMPs) and serine proteases from the plasmin system have attracted most attention,[2,8,9] the proteases involved in the reconstitution of the basement membrane, in the synthesis of the provisional extracellular matrix allowing cell migration, and, at later stages, in the formation of the mature scar tissue, have been studied to a much lesser extent. The main proteases involved in matrix protein maturation are the bone morphogenetic protein-1 (BMP-1)/tolloid-like proteinases (collectively called BTPs), a

small family of four metalloproteinases[10]: BMP-1, mammalian tolloid (mTLD), mammalian tolloid-like 1 (mTLL-1), and mammalian tolloid-like 2 (mTLL-2). Bone morphogenetic protein-1 and mTLD are alternatively spliced products of the same gene. In particular, these proteinases are involved in the proteolytic maturation of the fibrillar procollagens. In cornea, these include procollagens I and V, the most abundant components of corneal stroma, as well as procollagen III, a transient marker of the fibrotic evolution of corneal healing. More specialized roles in procollagen processing are played by the procollagen N-proteinase ADAMTS-2[11] and by the meprin proteinases, which have recently also been shown to be involved in propeptide processing of procollagens I and III.[12,13]

It is noteworthy that the BTPs are assisted during collagen maturation by two enhancing proteins, the procollagen C-proteinase enhancers (PCPE-1, PCPE-2), which lack intrinsic catalytic activity but can activate C-propeptide removal by BTPs by up to 20-fold.[14–16] Despite the prominent roles played by BMP-1/tolloid-like proteinases in collagen fibril formation, their direct implication in wound healing and scarring has never been studied. However, there is some evidence that BTPs could be involved in the excessive accumulation/disorganization of collagen fibrils that is the hallmark of fibrotic disease. For example, these enzymes have been found to be upregulated in a model of cardiac fibrosis,[17] and recombinant mTLD seems to promote renal fibrosis in rats with chronic kidney disease.[18] It has also recently been observed that human trabecular meshwork cells express BMP-1 in culture in which expression was increased when cells were of glaucomatous origin,[19] thereby possibly contributing to increased matrix stiffness.

In addition, PCPE-1 has also been found to be upregulated in a model of cardiac fibrosis,[20] as well as in carbon tetrachloride–induced liver fibrosis.[21] Furthermore, ablation of PCPE-2 expression in mouse results in decreased myocardial collagen accumulation in chronic pressure overload induced by transverse aortic constriction.[22]

Besides their role in collagen maturation, BTPs cleave a number of other proteins potentially important for collagen deposition, especially the pro-forms of lysyl oxidases involved in the formation of cross-links in collagen fibrils, and also several small leucine-rich proteoglycans (including decorin, biglycan, and mimecan/osteoglycin),[7,10,23] which associate with collagen fibrils and regulate their diameter and spacing. In addition, these proteinases are involved in basement membrane and anchoring filament assembly through the cleavage of laminin 332[24] and procollagen VII,[25] respectively. More recently, BMP-1/tolloid-like proteinases were shown to play a major role in the activation of TGF-β[26] and in the control of the angiogenic properties of perlecan,[27] two potentially important activities during corneal wound healing.

In view of these multiple substrates, it can be predicted that BTPs could be crucial in multiple aspects of wound healing. This, however, has never been experimentally demonstrated. In the present study, we monitored the expression of the various isoforms of these proteinases and their enhancers (PCPE-1 and -2) in normal and wounded mouse corneas. For the first time, the most important isoforms involved in corneal wound healing and scarring could be identified. Their expression was monitored up to 28 days post injury and was found to be very specific to the remodeling zone. In addition, we demonstrated strong immunostaining for BMP-1/mTLD and PCPE-1 in the injured areas of corneas from human patients, thereby confirming that BMP-1/tolloid-like proteinases and PCPEs are important players in corneal wound healing and could potentially participate in the development of stable corneal scars.

Materials and Methods

Animals and Corneal Scarring Model

C57BL/6 female mice aged from 12 to 16 weeks were used in this study. All experimental procedures were approved by the Ethical Committee of the Centre of Physiopathology Toulouse Purpan and conducted in accordance with the ARVO Statement for the Use of Animals in Ophthalmic and Vision Research.

Anesthesia was performed by intraperitoneal injection of 20 mg/kg ketamine hydrochloride (Panpharma, Luitré, France) and 8.8 mg/kg xylazine hydrochloride (Bayer Healthcare, Loos, France). Before surgery, atropine sulfate ophthalmic solution 1% (Alcon Laboratories, Inc., Fort Worth, TX, USA), as well as 0.4% oxybuprocaine (Novartis Pharma Schweiz AG, Rotkreuz, Switzerland), was applied topically. Euthanasia was performed after inhalation of isoflurane, followed by dislocation of cervical vertebrae. All surgical procedures were performed by the same surgeon to ensure consistency across specimens.

The murine full-thickness excision model was adapted from the penetrating keratectomy model described by Stramer et al.[28] Surgery was performed on the left eyes. Briefly, a 0.75-mm full-thickness button of central cornea tissue including all three corneal tissue layers (epithelium, stroma, and endothelium) was ablated. A 26-gauge needle was used to mark the area that was then removed with microdissecting scissors.

The animals were then euthanized at specific intervals of healing (day 7, 14, 21, or 28). Each left eye was removed and embedded in Tissue-Tek optimum cutting temperature (OCT) compound (Sakura Finetek Europe B.V., Zoeterwoude, The Netherlands) for histology procedures. Alternatively, the left eyes were dissected to collect the corneal epithelium and corneal stroma for mRNA extraction and subsequent RT-quantitative (Q)-PCR analysis. Control samples were collected from left and right eyes of mice, following the same experimental procedure (anesthesia, atropine, oxybuprocaine), but no surgery was performed.

Human Corneas

Five corneas were included in this study: Four human corneas presenting permanent stromal scars were collected after transplantation, and one normal human cornea obtained after enucleation for melanoma was also collected. Control cornea was processed within 6 hours after death and immediately after enucleation. Table 1 summarizes clinical conditions and parameters of the different corneas.

Datas on cornea from patients P1, P2, and C1 were previously published, and we discussed that in the case of P2, this type of condition presented traumatic areas following the infectious phase, with presence of alpha smooth muscle–positive cells.[29] Corneas were embedded in Tissue-Tek OCT compound (Sakura Finetek Europe B.V.) just after surgery. Corneal samples were intended for destruction after surgery. This study adhered to the tenets of the Declaration of Helsinki.

Electron Microscopy

For transmission electron microscopy, corneas were first briefly rinsed twice in PBS and then fixed overnight at room temperature in 2.5% glutaraldehyde and 2% paraformaldehyde in 0.1 M sodium cacodylate pH 7.4. After a few washes in 0.1 M sodium cacodylate pH 7.4, specimens were postfixed in 1% osmium tetroxide 0.1 M cacodylate pH 7.4 for 45 minutes, then dehydrated in a graded ethanol series (30%–100%) and embedded in epoxy resin. To locate areas of interest, semithin sections (0.3 μm) stained with methylene blue/Azur II were

Table 1. Description of Human Corneas

Number	Age	Sex	Etiology	Age of Scar, y	Scar Characteristics
P1	40	M	Physical trauma, barbed wire	1.5	Central opacity, all stromal depth, perforating trauma
P2	22	F	Herpetic keratitis	5	Central anterior stroma opacity
P3	36	M	Physical trauma, tree branch	14	Complete stromal opacity, all stromal depth, perforating trauma
P4	38	F	Physical trauma, knife	24	Central anterior opacity, perforating trauma
C1	75	M	No history of corneal pathology		

first observed histologically using a Leica (Wetzlar, Germany) light microscope equipped with a digital camera (Nikon, Champigny sur Marne, France). Ultrathin 65-nm sections were stained with uranyl acetate and lead citrate and then examined in a Philips (Suresnes, France) CM120 electron microscope equipped with a GATAN Orius 200 2Kx2K digital camera (Centre Technique des Microstructures, Université Claude Bernard Lyon I, Villeurbanne, France). Collagen fibril diameters were measured with ImageJ software (National Institute of Mental Health, Bethesda, MD, USA), selecting fibrils in (near) transverse section using the ellipse function, with the minimum dimension used as a measure of fibril diameter.

Immunohistochemistry

The following antibodies and dilutions were used. Mouse samples: rat monoclonal IgG1 anti-mouse PCPE-1 (MAB2239; R&D Systems, Minneapolis, MN, USA) 1:100, AlexaFluor 555 goat anti-rat IgG 1:400 (Invitrogen Molecular Probes, Eugene, OR, USA), rat monoclonal IgG2b anti-human BMP-1 (MAB1927; R&D Systems) 1:100, rat IgG1 isotype control (MAB005; R&D Systems), rat IgG2b isotype control (MAB0061; R&D Systems), and rabbit serum (R9133; Sigma, Saint-Quentin Fallavier, France). Human samples: rat monoclonal IgG2b anti-human BMP-1 (MAB1927; R&D Systems) 1:100, rabbit polyclonal IgG anti-human PCPE-1 (P6243; Sigma) 1:200, and AlexaFluor 546 goat anti-rabbit IgG (Invitrogen Molecular Probes) 1:400.

Briefly, corneal cryostat sections (7–10 μm thick) were used. Samples were fixed with paraformaldehyde 4% at 4°C, then permeabilized with Triton X-100. Primary and secondary antibodies were incubated for 2 and 1 hour(s), respectively, at room temperature in a humidified dark chamber. No primary antibody or appropriate isotype control immunolabeling was performed at the same time. Final mounting of tissue sections was performed with ProLong Gold antifade reagent with 4′,6-diamidino-2-phenylindole (DAPI; Molecular Probes). Sections were observed 24 hours later, using the ×10 or ×40 objective of a Leica DMR microscope. Images were acquired using a Leica DFC 300 FX camera and IM50 software (Leica) at 400 ms for the ×10 objective and 260 ms for the ×40 objective. These exposure times were determined from the control conditions (unwounded) and applied to the other samples.

Alpha smooth muscle actin (αSMA) staining was performed as previously described.[29]

Reverse Transcriptase–Real-Time Polymerase Chain Reaction

Total RNA was extracted using the Qiagen MicroRNA extraction kit according to the manufacturer's recommendations (Qiagen, Valencia, CA, USA). The RNA integrity number (RIN) was determined with an Agilent 2000 nanochip kit (Agilent, Waldbronn, Germany). Each sample used had an RIN of at least 7.

Reverse transcriptase–PCR was performed using the Invitrogen Superscript III VILO kit according to the manufacturer's recommendations (Invitrogen, Carlsbad, CA, USA). Real-time PCR was performed on 50 pg cDNA in a Roche LightCycler 480 using Roche supermix for PCR (Roche, Boulogne-Billancourt, France). Polymerase chain reaction efficiency was determined for each primer set to calculate the expression ratio. For the stroma, normalization was performed using three housekeeping genes (vimentin, tyrosine 3 monooxygenase, β2-microglobulin), as previously described.[30] Primer sequences were BMP-1/mTLD (F: GTCTAT GAAGCCATTTGCGG, R: GACGCTCAATCTCAAAGGAC), PCPE-1 (F: CTCAAACCAGGTGATCATGC, R: AGAGATGGGGC TAGGGGCCT), PCPE-2 (F: CGCCAGAGAGACCTGTTTTC, R: CCTCAGGAACTGTGATTTTC), TLL-1 (F: GGCTGGAGTTCTTA CATCTACG, R: CTTATCTCCCCTCCACAAATCG), TLL-2 (F: GTA TATGAAGCCATGTGTGG, R: GCCTTTCGATCTCGAAGGAC), COL1A1 (F: CGGCTCCTGCTCCTCTTAG, R: CTGTCCAGG GATGCCATCT), COL3A1 (F: GGCCCTCCTGGTATTCCTG, R: GCCAATTCCTCCTATGCCAG), vimentin (F: CAAGTC CAAGTTTGCTGACC, R: CTCCGGTACTCGTTTGACTC), tyrosine 3 mono-oxygenase (F: TGGATAAGAGTGAGCTGGTACA, R: CGTGTCCCTGCTCTGTTACG), β2-microglobulin (F: TTCTGGTGCTTGTCTCACTGA, R: CAGTATGTTCGGCTTCC CATTC). For the epithelium, we used three other housekeeping genes for normalization as previously described[29]: ubiquitin C (F: AACCCACAGTATATCTTTGGCG, R: CCCTCACTAGGTTCGAT GACTTC), tatabox (F: TGCCGAAAGATGCACAGATGA, R: TGTTGTCACATATCGGAAGGC), and β-actin (F: CGGTCCACCCGCCACCAGTTCGCCA, R: TCCCACCATCA CACCCTGGTGCCTA). The fold change in gene expression was calculated using the 2 ΔΔCT ratio according to a previously described method.[31] All PCR products were checked by sequencing (Millegen, Toulouse, France).

Statistical Analysis

For all experiments, group-to-group comparisons were performed using a nonparametric Wilcoxon test.

Results

Wound healing was followed in mouse corneas after full-thickness excision, using the model described by Stramer et al.[28] As previously described,[29,30] by microscopic examination, histology, and immunolabeling for αSMA, this model shows scar formation with differentiation of keratocytes into myofibroblasts and maximum corneal opacity occurring 14 days post surgery. Opacity could still be observed at least 7 months post injury.

We also examined control and wounded corneas (day 14) by transmission electron microscopy (Fig. 1). In control corneas, the epithelial basement membrane was well defined and was associated with numerous hemidesmosomes underlying epithelium (Fig. 1A). The stroma showed the typical multilayer organization (Fig. 1C) with collagen fibrils, of 27.4 ± 3.9-nm ($n = 288$) uniform diameter (Fig. 1E), interspersed by extended quiescent keratocytes. In the wounded corneas, both the epithelium and endothelium had reformed well (not shown). There was also an almost continuous basement

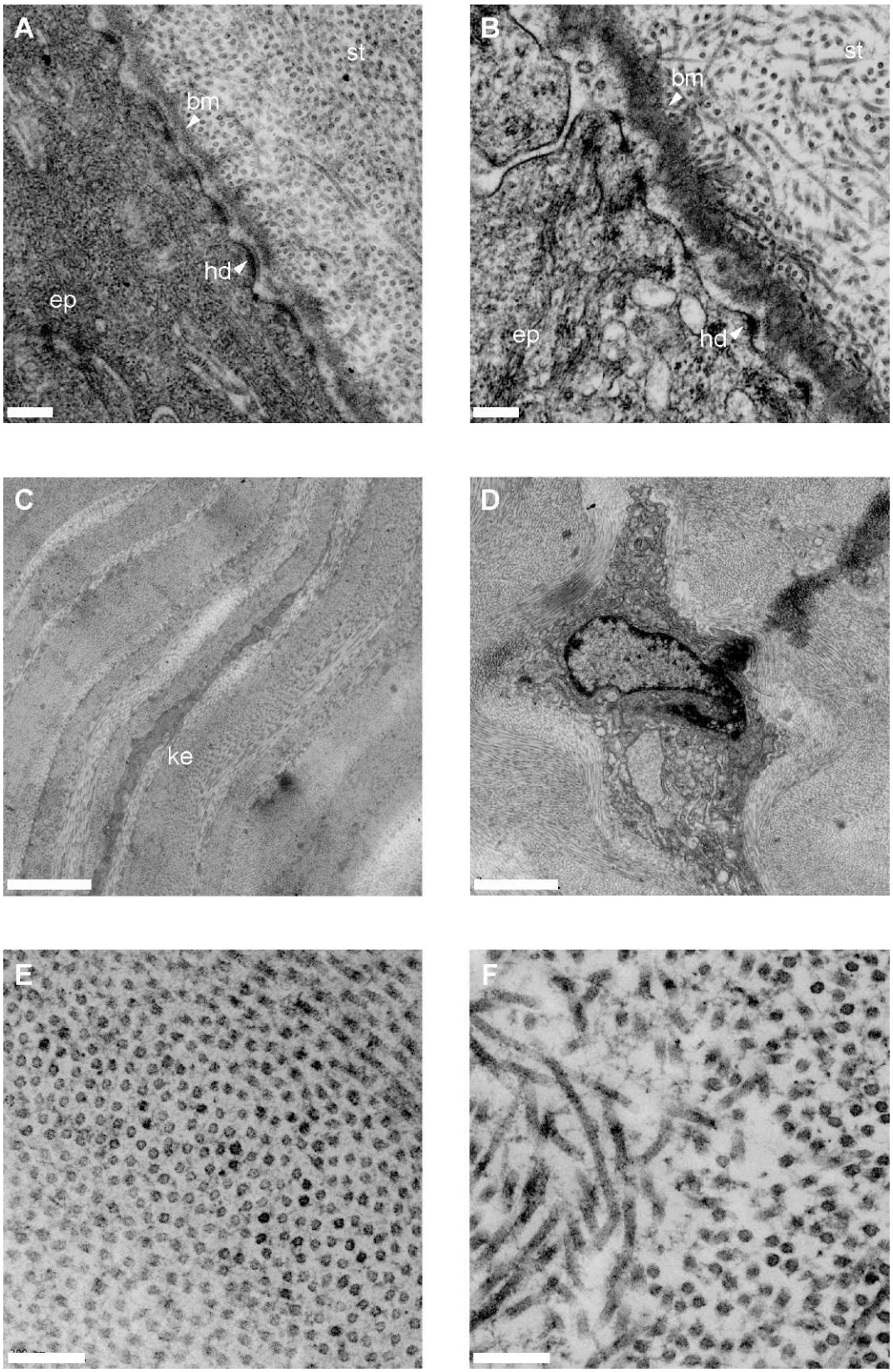

Figure 1. Transmission electron microscopy of control (**A**, **C**, **E**) and wounded corneas (**B**, **D**, **F**), the latter 14 days after surgery. (**A**, **B**) Epithelial basement membrane region, showing the epithelium (ep), stroma (st), basement membrane (bm), and hemidesmosomes (hd). *Scale bars*: 200 nm. (**C**, **D**) Stroma, showing collagen fibrils and a keratocyte (ke). *Scale bars*: 2 μm. (**E**, **F**) High-magnification view of collagen fibrils in the stroma. *Scale bars*: 200 nm.

Investigative Ophthalmology & Visual Science

Table 2. Messenger RNA Expression Levels in Mouse Corneal Epithelium and Stroma, Normalized to a Set of Housekeeping Genes (HKG), for Control (Unwounded) and Wounded Corneas up to 28 Days Post Surgery

	mRNA Expression Levels, % HKG (±SEM)				
Name	**Control**	**7 d**	**14 d**	**21 d**	**28 d**
Epithelium					
BMP-1/mTLD	3.07 (0.1)	8.78 (1.26)*	11.58 (2.89)*	7.86 (1.32)*	3.98 (0.62)
TLL-1	<0.03	<0.03	<0.03	<0.03	<0.03
TLL-2	NA	NA	NA	NA	NA
PCPE-1	8.47 (0.32)	9.06 (1.96)	13.18 (1.47)*	17.24 (2.49)*	13.61 (1.59)*
PCPE-2	4.39 (0.21)	1.25 (0.48)*	0.72 (0.15)*	0.90 (0.23)*	1.41 (0.34)*
Stroma					
BMP-1/mTLD	4.05 (0.32)	6.25 (0.66)*	5.87 (0.56)*	4.61 (0.53)	5.12 (0.24)*
TLL-1	<0.03	<0.03	<0.03	<0.03	<0.03
TLL-2	NA	NA	NA	NA	NA
PCPE-1	19.88 (1.11)	25.88 (2.62)	27.96 (1.88)*	27.17 (2.93)*	30.84 (2.59)*
PCPE-2	5.76 (0.67)	1.09 (0.13)*	2.57 (0.41)*	1.94 (0.46)*	1.95 (0.44)*

* Significant changes ($P < 0.05$).

membrane, which in some areas seemed somewhat diffuse compared to that in control corneas (Fig. 1B). The collagen fibrils in the stroma of the wounded corneas were relatively disorganized and less tightly packed, and there was widespread cellular infiltration and keratocyte activation (Fig. 1D). In contrast, there were no significant differences, compared to control corneas, in the appearance or diameter of the collagen fibrils (diameter 28.1 ± 3.9 nm, $n = 245$; Fig. 1F).

In initial studies by Q-PCR on control corneas, expression of BMP-1/mTLD and mTLL-1 was detected in both epithelium and stroma (Table 2). Expression of mTLL-1 was relatively weak, however, while mTLL-2 was not detected at all. In addition, both PCPE-1 and PCPE-2 were detected in both epithelium and stroma. In control stroma, PCPE-1 mRNA levels were 4-fold higher than levels of PCPE-2 mRNA, and approximately 5-fold higher than for BMP-1/mTLD. In control epithelium, PCPE-1 was still the most expressed mRNA with levels approximately 2-fold higher than for PCPE-2 and approximately 3-fold higher than for BMP-1/mTLD.

As previously described,[29,30] we used type III collagen expression as a positive marker of scar formation. Here we found that collagen III expression remained high throughout the follow-up period after surgery, starting to decrease at 28 days (Fig. 2A).

Bone morphogenetic protein-1/mTLD stromal expression was significantly increased by factors of 1.61 ± 0.17, 1.51 ± 0.15, and 1.36 ± 0.05, respectively, at days 7, 14, and 28 after wounding ($P < 0.01$, Fig. 2B). Expression of PCPE-1 in the stroma was also consistently increased, by factors of 1.44 ± 0.08, 1.40 ± 0.15, and 1.63 ± 0.14 at days 14, 21, and 28, respectively ($P < 0.01$, Fig. 2B). Surprisingly, expression of PCPE-2 (albeit starting from a relatively low level; Table 2) was markedly reduced by factors of 0.21 ± 0.03, 0.50 ± 0.08, 0.38 ± 0.09, and 0.42 ± 0.08 of control levels at days 7 to 28 ($P < 0.001$, Fig. 2B). It should be noted that entire stroma were used for the Q-PCR analysis, including both the wound region and the surrounding tissue.

Similar changes in expression were seen in the corneal epithelium, though the increase in BMP-1/mTLD expression was much greater than in the stroma (Fig. 2C). Bone morphogenetic protein-1/mTLD expression was significantly increased by factors of 3.00 ± 0.65, 3.83 ± 0.96, and 2.60 ± 0.44 at days 7, 14, and 21, respectively ($P < 0.001$, Fig. 2C). Expression of PCPE-1 was also significantly increased by factors of 1.59 ± 0.18, 2.08 ± 0.30, and 1.64 ± 0.19 at days 14, 21, and 28, respectively ($P < 0.001$, Fig. 2C). As in the stroma, PCPE-2 expression was significantly decreased by factors of 0.30 ± 0.11, 0.17 ± 0.04, 0.21 ± 0.05, and 0.33 ± 0.08 of control levels at days 7 to 28 ($P < 0.0001$, Fig. 2C).

By immunohistochemistry, relatively high levels of BMP-1/mTLD protein were detected in the epithelium of control corneas, with only weak labeling in the stroma (Fig. 3A). Seven days after surgery, there was a strong increase in BMP-1/mTLD expression in the stroma that was localized to the wound area (Fig. 3B) and persisted until days 21 and 28, albeit to a lower extent (Figs. 3C, 3D). Throughout the follow-up period, expression of BMP-1/mTLD in the epithelium remained strong.

For PCPE-1 (Fig. 3E), there was only weak labeling in the stroma of control corneas. Following surgery, as for BMP1/mTLD, there was a strong increase in protein expression, confined to the wound area of the stroma, at day 7 (Fig. 3F). Expression of PCPE-1 remained high throughout days 21 and 28 (Figs. 3G, 3H). Finally, there was no detectable expression of PCPE-1 protein in the epithelium, in contrast to the results from Q-PCR analysis (see above).

Finally, we asked whether BMP-1/tolloid-like proteinases were also upregulated in corneal scarring in human pathologies (Fig. 4). Several types of lesion were investigated: mechanical traumas (P1, P3, and P4) and following herpetic keratitis (P2). All mechanical traumas were perforating. The P2 cornea was affected by herpetic keratitis and was used to evaluate the consequences of persistent inflammation on the expression of BMP-1/mTLD and PCPE-1. As in the mouse model, increased expression of both BMP-1 and PCPE-1 was seen in the scar area in all cases (white arrows point toward the wound area). Interestingly, in contrast with our observations in mouse corneas, PCPE-1 immunostaining was also seen in the epithelium of human corneas.

Discussion

Here we show, for the first time, that corneal repair is associated with an upregulation, in the wound region, of the expression of both BMP-1/mTLD proteinase and its enhancer PCPE-1. Considering their substrate specificity toward extracellular matrix components, such an upregulation would be expected for the reconstitution of the extracellular matrix following injury. However, the extent to which this contributes to the observed corneal scar is unclear. Various phenomena are thought to contribute to the appearance of corneal scarring.[32–35] One factor is the increased light scattering due to the

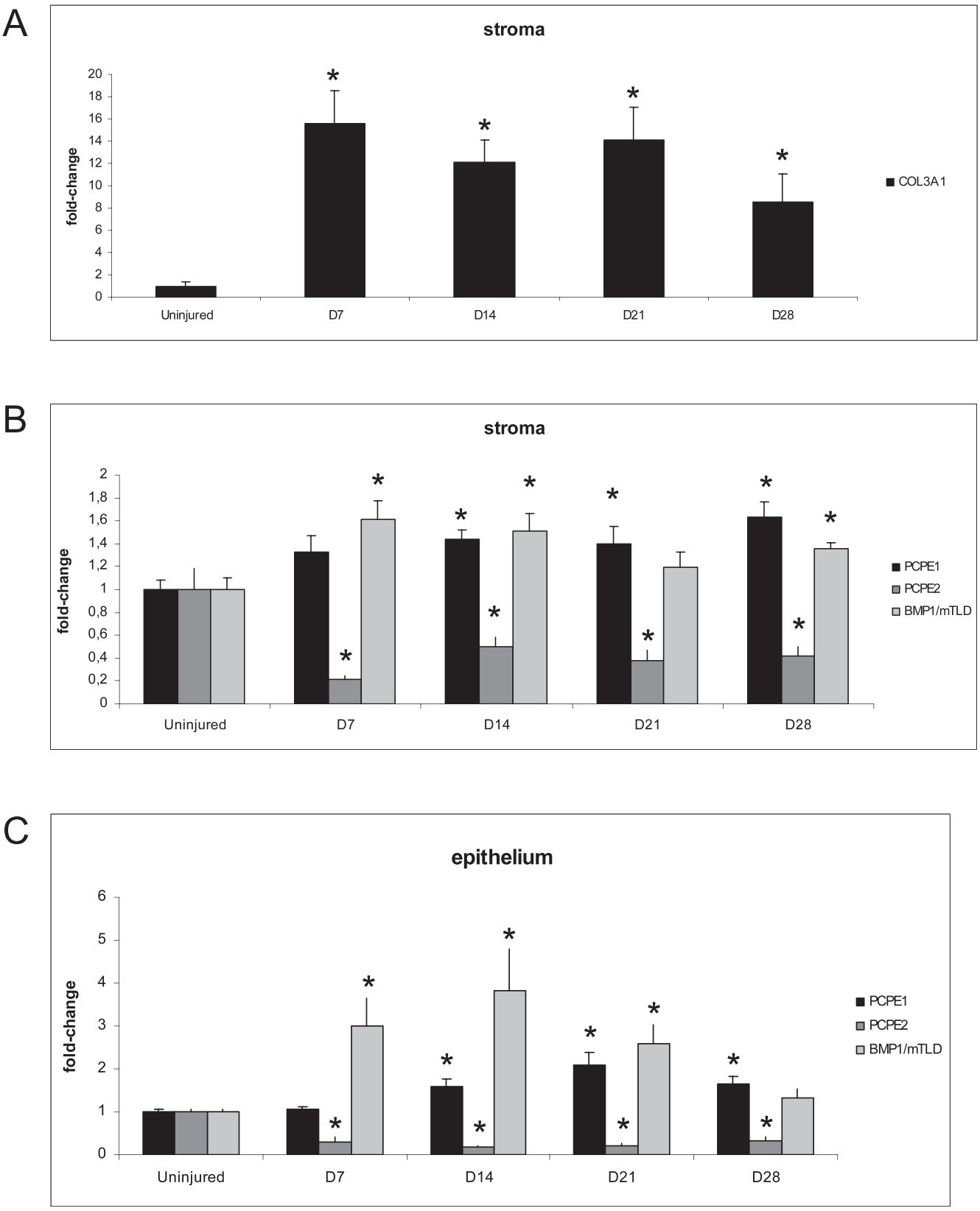

Figure 2. Quantitative-PCR analysis of fold change in gene expression in the stroma (**A**, **B**) and (**C**) epithelium during mouse corneal wound repair. (**A**) Collagen III, (**B**, **C**) BMP-1/mTLD, PCPE-1, and PCPE-2. Significant changes ($P < 0.05$) are indicated by *asterisk*.

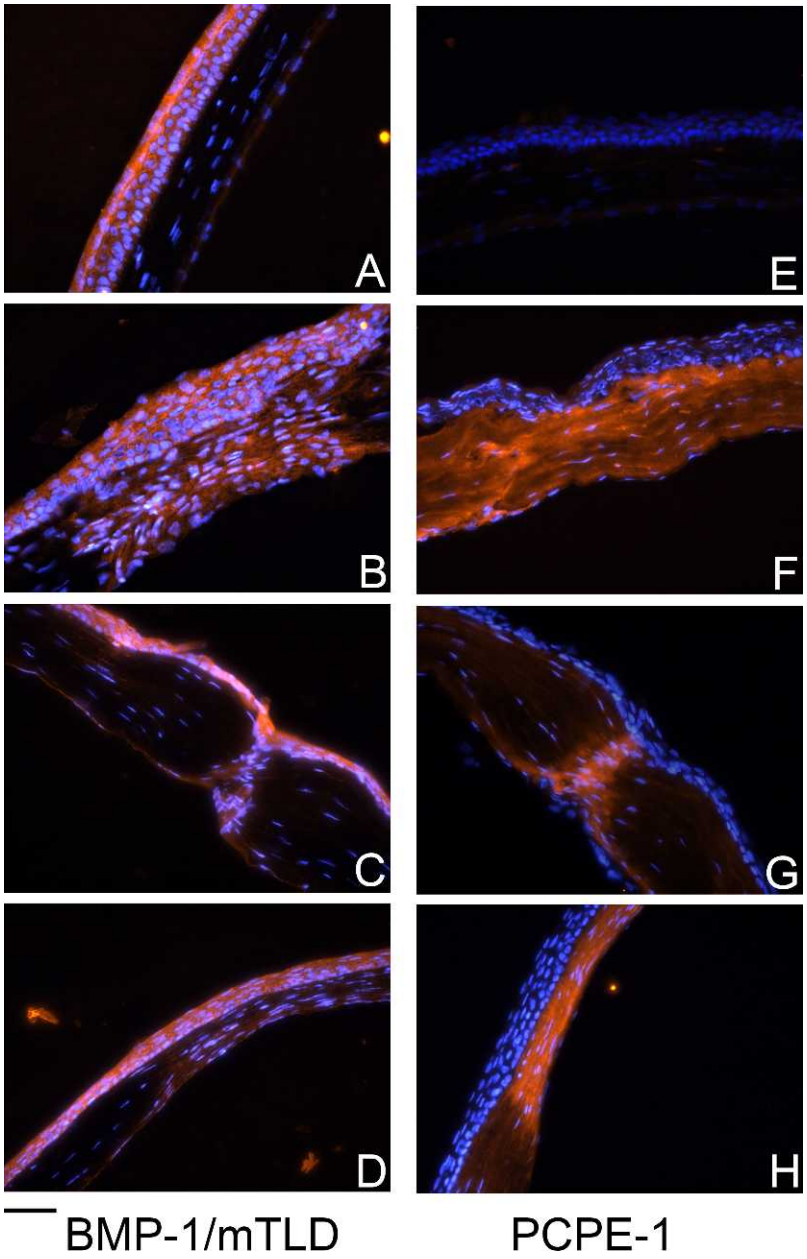

FIGURE 3. Immunohistochemistry of BMP-1/mTLD (**A–D**) and PCPE-1 (**E–H**) expression in control (**A–E**) and wounded corneas, the latter at days 7 (**B**, **F**), 21 (**C**, **G**), and 28 (**D**, **H**), respectively. DAPI-staining nuclei in *blue*. *Scale bar*: 25 μm.

presence of inflammatory cells and activated keratocytes, involving changes in cell crystallins that alter their refractive properties.[33] In the mouse model described here, keratocyte differentiation into myofibroblasts was previously demonstrated by the expression of αSMA,[29,30] and the electron microscopy analysis carried out here also shows clear evidence of cellular infiltration into the wound zone. Differentiation of corneal keratocytes into myofibroblasts is triggered by TGF-β; and since BMP-1 is known to be involved in the activation of TGF-β,[26] this is one way in which overexpression of BMP-1/mTLD could contribute to corneal scar.

Another factor contributing to scarring is the increased disorganization of the normally highly organized stromal collagen network that results in increased destructive interference of scattered light and hence reduced transparency.[35–37] This might involve increase in collagen fibril diameter and in the interfibrillar spacing, both of which are regulated by the small leucine-rich proteoglycans (including lumican, keratocan, mimecan/osteoglycin, decorin, and biglycan in the cornea[38]). Changes in the relative proportions of these proteoglycans during corneal wound healing in a rabbit model have been observed.[39] In addition, increased corneal thickness and amount of extracellular matrix deposition, including collagen, could also increase scattering, though again in the rabbit model there is no evidence of excessive collagen deposition.[40,41] In the observations reported here using the mouse model, there were no differences in fibril diameter compared to controls. There was, however, increased disorganization of the collagen fibrils, probably in relation to the upregulation of BMP-1, which is known to intervene at several levels in collagen fibril assembly[7,10] (procollagen processing, proteoglycan maturation, lysyl oxidase–induced cross-linking).

All in all, there are a number of ways by which increased BMP-1 and PCPE-1 expression might lead to corneal scarring.

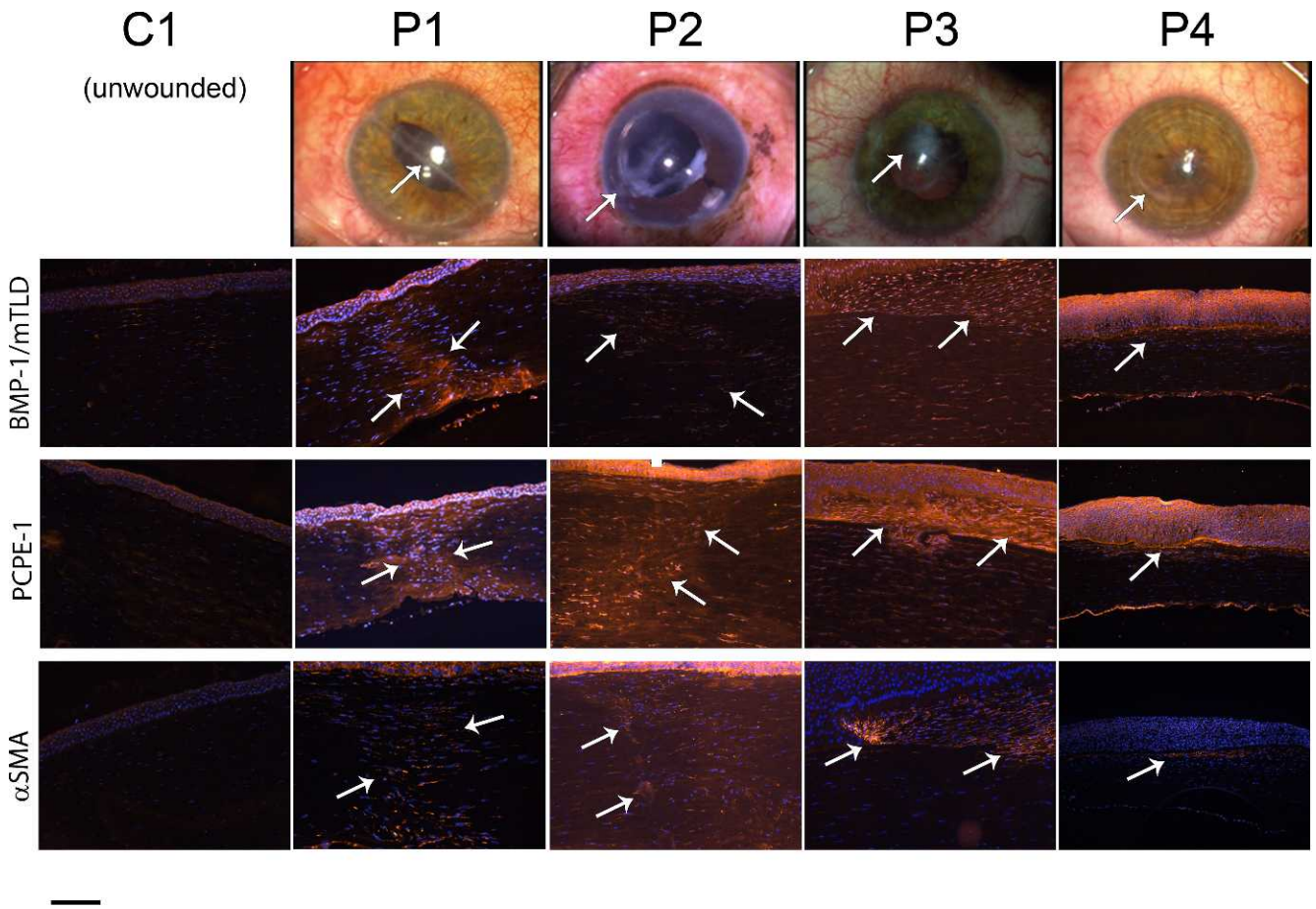

FIGURE 4. Expression of BMP-1/mTLD and PCPE-1 in human corneal lesions. BMP1/mTLD, PCPE1, and αSMA in *red*, DAPI-staining nuclei in *blue*. *Scale bar*: 100 μm.

Further studies are required (currently in progress) using specific inhibitors and gene inactivation to study the effects of reducing proteolytic activity through this proteinase/enhancer system.

The relatively strong expression of BMP-1 in the corneal epithelium is intriguing. Since control corneas also display strong BMP-1/mTLD immunostaining, it seems likely that BMP-1/mTLD plays a role in corneal epithelial homeostasis. Somewhat different observations have been made in fetal and adult skin, where BMP-1/mTLD expression is found mainly in the basal layer of the epidermis.[24,25] Such an epithelial localization would be consistent with the known roles of BMP-1 in cleavage of the basement membrane proteins perlecan[27] and laminin 332,[24,42] as well as in the processing of procollagen VII leading to the formation of anchoring fibrils linking the basement membrane to the underlying dermis.[25] Surprisingly, while previous studies[43] have shown that human skin keratinocytes do not express PCPE-1, we report here mRNA expression for PCPE-1 in the corneal epithelium. These observations also differ from our immunohistochemical data in mice, which show expression of BMP-1/mTLD, but not PCPE-1, in the epithelium. This difference is probably due to poor antibody sensitivity.

Expression of PCPE-1 mRNA in the cornea was found to increase during wound healing. However, expression of PCPE-2, albeit present at much lower levels than PCPE-1 in normal cornea, is decreased. Previous studies suggest that PCPE-1 and -2 show tissue-specific expression.[15,44] Our data strengthen these observations and suggest that PCPE-1 is corneal specific, while PCPE-2 could be specific to other tissues/functions with, for example, a prominent role in lipid metabolism.[45]

Finally, we confirmed that BMP-1/mTLD and PCPE-1 overexpression was also found in humans. Several studies have previously identified these proteins in normal corneas.[46–48] We confirmed and observed a weak expression in the unwounded human cornea. In contrast, we observed that both BMP-1/mTLD and PCPE-1 expression were increased in the stromal scar areas and in inflammatory situations (here herpetic keratitis). This suggests that BMP-1/mTLD and PCPE-1 are as active in human scars as they are during mouse corneal repair. While the precise mechanisms involved remain to be elucidated, the clear association of BMP-1/mTLD and PCPE-1 with corneal scarring in both the mouse and human situations suggests that these proteins may represent future therapeutic targets.

Acknowledgments

We thank Marie-Andrée Daussion and Jérôme Bernard from the Centre de Recherche de Chirurgie Expérimentale Claude Bernard (Centre Hospitalier Universitaire, Purpan, Toulouse, France) for animal care and experiments. We also thank Talal Al Saati and Florence Capilla from the histopathology core facility for their technical assistance (Anexplo/GenoToul; UMS 06). Finally, we thank Angélique Erraud for her work on our team these past 5 years.

Supported by the Agence Nationale de la Recherche (ANR-07-PHYSIO-022-01), the Région Rhône-Alpes, the Centre National de la Recherche Scientifique, the Fondation de l'Avenir (ET0-594, ET7-

474, ET3-701), the Fondation de France (Grants Berthe Fouassier 2009002318 and 2009002320), the Fondation des Aveugles de Guerre, the Région Midi-Pyrénées, the Université Claude Bernard Lyon 1 and the Université Paul Sabatier Toulouse 3.

Disclosure: **F. Malecaze**, None; **D. Massoudi**, None; **P. Fournié**, None; **C. Tricoire**, None; **M. Cassagne**, None; **M. Malbouyres**, None; **D.J.S. Hulmes**, None; **C. Moali**, None; **S.D. Galiacy**, None

References

1. Dawson DG, Edelhauser HF, Grossniklaus HE. Long-term histopathologic findings in human corneal wounds after refractive surgical procedures. *Am J Ophthalmol*. 2005;139: 168–178.
2. Fini ME, Stramer BM. How the cornea heals: cornea-specific repair mechanisms affecting surgical outcomes. *Cornea*. 2005; 24:S2–S11.
3. Foster A, Resnikoff S. The impact of Vision 2020 on global blindness. *Eye (Lond)*. 2005;19:1133–1135.
4. Jester JV, Petroll WM, Cavanagh HD. Corneal stromal wound healing in refractive surgery: the role of myofibroblasts. *Prog Retin Eye Res*. 1999;18:311–356.
5. Saika S, Yamanaka O, Sumioka T, et al. Fibrotic disorders in the eye: targets of gene therapy. *Prog Retin Eye Res*. 2008;27:177–196.
6. Wilson SE, Mohan RR, Mohan RR, Ambrosio R Jr, Hong J, Lee J. The corneal wound healing response: cytokine-mediated interaction of the epithelium, stroma, and inflammatory cells. *Prog Retin Eye Res*. 2001;20:625–637.
7. Moali C, Hulmes DJ. Extracellular and cell surface proteases in wound healing: new players are still emerging. *Eur J Dermatol*. 2009;19:552–564.
8. Twining SS, Wilson PM, Ngamkitidechakul C. Extrahepatic synthesis of plasminogen in the human cornea is up-regulated by interleukins-1alpha and -1beta. *Biochem J*. 1999;339(pt 3): 705–712.
9. Watanabe M, Yano W, Kondo S, et al. Up-regulation of urokinase-type plasminogen activator in corneal epithelial cells induced by wounding. *Invest Ophthalmol Vis Sci*. 2003; 44:3332–3338.
10. Hopkins DR, Keles S, Greenspan DS. The bone morphogenetic protein 1/Tolloid-like metalloproteinases. *Matrix Biol*. 2007; 26:508–523.
11. Porter S, Clark IM, Kevorkian L, Edwards DR. The ADAMTS metalloproteinases. *Biochem J*. 2005;386:15–27.
12. Kronenberg D, Bruns BC, Moali C, et al. Processing of procollagen III by meprins: new players in extracellular matrix assembly? *J Invest Dermatol*. 2010;130:2727–2735.
13. Broder C, Arnold P, Vadon-Le Goff S, et al. Metalloproteases meprin alpha and meprin beta are C- and N-procollagen proteinases important for collagen assembly and tensile strength. *Proc Natl Acad Sci U S A*. 2013;110:14219–14224.
14. Adar R, Kessler E, Goldberg B. Evidence for a protein that enhances the activity of type I procollagen C-proteinase. *Coll Relat Res*. 1986;6:267–277.
15. Steiglitz BM, Keene DR, Greenspan DS. PCOLCE2 encodes a functional procollagen C-proteinase enhancer (PCPE2) that is a collagen-binding protein differing in distribution of expression and post-translational modification from the previously described PCPE1. *J Biol Chem*. 2002;277:49820–49830.
16. Bourhis JM, Vadon-Le Goff S, Afrache H, et al. Procollagen C-proteinase enhancer grasps the stalk of the C-propeptide trimer to boost collagen precursor maturation. *Proc Natl Acad Sci U S A*. 2013;110:6394–6399.
17. Kobayashi K, Luo M, Zhang Y, et al. Secreted Frizzled-related protein 2 is a procollagen C proteinase enhancer with a role in fibrosis associated with myocardial infarction. *Nat Cell Biol*. 2009;11:46–55.
18. Grgurevic L, Macek B, Healy DR, et al. Circulating bone morphogenetic protein 1-3 isoform increases renal fibrosis. *J Am Soc Nephrol*. 2011;22:681–692.
19. Tovar-Vidales T, Fitzgerald AM, Clark AF, Wordinger RJ. Transforming growth factor-beta2 induces expression of biologically active bone morphogenetic protein-1 in human trabecular meshwork cells. *Invest Ophthalmol Vis Sci*. 2013; 54:4741–4748.
20. Kessler-Icekson G, Schlesinger H, Freimann S, Kessler E. Expression of procollagen C-proteinase enhancer-1 in the remodeling rat heart is stimulated by aldosterone. *Int J Biochem Cell Biol*. 2006;38:358–365.
21. Ogata I, Auster AS, Matsui A, et al. Up-regulation of type I procollagen C-proteinase enhancer protein messenger RNA in rats with CCl4-induced liver fibrosis. *Hepatology*. 1997;26: 611–617.
22. Baicu CF, Zhang Y, Van Laer AO, Renaud L, Zile MR, Bradshaw AD. Effects of the absence of procollagen C-endopeptidase enhancer-2 on myocardial collagen accumulation in chronic pressure overload. *Am J Physiol Heart Circ Physiol*. 2012;303: H234–H240.
23. von Marschall Z, Fisher LW. Decorin is processed by three isoforms of bone morphogenetic protein-1 (BMP1). *Biochem Biophys Res Commun*. 2010;391:1374–1378.
24. Amano S, Scott IC, Takahara K, et al. Bone morphogenetic protein 1 is an extracellular processing enzyme of the laminin 5 gamma 2 chain. *J Biol Chem*. 2000;275:22728–22735.
25. Rattenholl A, Pappano WN, Koch M, et al. Proteinases of the bone morphogenetic protein-1 family convert procollagen VII to mature anchoring fibril collagen. *J Biol Chem*. 2002;277: 26372–26378.
26. Ge G, Greenspan DS. BMP1 controls TGFbeta1 activation via cleavage of latent TGFbeta-binding protein. *J Cell Biol*. 2006; 175:111–120.
27. Gonzalez EM, Reed CC, Bix G, et al. BMP-1/tolloid-like metalloproteases process endorepellin, the angiostatic C-terminal fragment of perlecan. *J Biol Chem*. 2005;280:7080–7087.
28. Stramer BM, Zieske JD, Jung JC, Austin JS, Fini ME. Molecular mechanisms controlling the fibrotic repair phenotype in cornea: implications for surgical outcomes. *Invest Ophthalmol Vis Sci*. 2003;44:4237–4246.
29. Massoudi D, Malecaze F, Soler V, et al. NC1 long and NC3 short splice variants of type XII collagen are overexpressed during corneal scarring. *Invest Ophthalmol Vis Sci*. 2012;53:7246–7256.
30. Galiacy SD, Fournie P, Massoudi D, et al. Matrix metalloproteinase 14 overexpression reduces corneal scarring. *Gene Ther*. 2011;18:462–468.
31. Vandesompele J, De Preter K, Pattyn F, et al. Accurate normalization of real-time quantitative RT-PCR data by geometric averaging of multiple internal control genes. *Genome Biol*. 2002;3:research0034.1–research0034.11.
32. Hassell JR, Birk DE. The molecular basis of corneal transparency. *Exp Eye Res*. 2010;91:326–335.
33. Jester JV. Corneal crystallins and the development of cellular transparency. *Semin Cell Dev Biol*. 2008;19:82–93.
34. McCally RL, Freund DE, Zorn A, et al. Light-scattering and ultrastructure of healed penetrating corneal wounds. *Invest Ophthalmol Vis Sci*. 2007;48:157–165.
35. Meek KM, Leonard DW, Connon CJ, Dennis S, Khan S. Transparency, swelling and scarring in the corneal stroma. *Eye (Lond)*. 2003;17:927–936.
36. Connon CJ, Marshall J, Patmore AL, Brahma A, Meek KM. Persistent haze and disorganization of anterior stromal

Investigative Ophthalmology & Visual Science

collagen appear unrelated following phototherapeutic keratectomy. *J Refract Surg*. 2003;19:323–332.

37. Rawe IM, Meek KM, Leonard DW, Takahashi T, Cintron C. Structure of corneal scar tissue: an X-ray diffraction study. *Biophys J*. 1994;67:1743–1748.
38. Knupp C, Pinali C, Lewis PN, et al. The architecture of the cornea and structural basis of its transparency. *Adv Protein Chem Struct Biol*. 2009;78:25–49.
39. Cintron C, Gregory JD, Damle SP, Kublin CL. Biochemical analyses of proteoglycans in rabbit corneal scars. *Invest Ophthalmol Vis Sci*. 1990;31:1975–1981.
40. Cintron C, Hong BS, Kublin CL. Quantitative analysis of collagen from normal developing corneas and corneal scars. *Curr Eye Res*. 1981;1:1–8.
41. Cintron C, Schneider H, Kublin C. Corneal scar formation. *Exp Eye Res*. 1973;17:251–259.
42. Veitch DP, Nokelainen P, McGowan KA, et al. Mammalian tolloid metalloproteinase, and not matrix metalloprotease 2 or membrane type 1 metalloprotease, processes laminin-5 in keratinocytes and skin. *J Biol Chem*. 2003;278:15661–15668.
43. Lee S, Solow-Cordero DE, Kessler E, Takahara K, Greenspan DS. Transforming growth factor-beta regulation of bone morphogenetic protein-1/procollagen C-proteinase and related proteins in fibrogenic cells and keratinocytes. *J Biol Chem*. 1997;272:19059–19066.
44. Heinzel K, Bleul CC. The Foxn1-dependent transcripts PCOLCE2 and mPPP1R16B are not required for normal thymopoiesis. *Eur J Immunol*. 2007;37:2562–2571.
45. Francone OL, Ishida BY, de la Llera-Moya M, et al. Disruption of the murine procollagen C-proteinase enhancer 2 gene causes accumulation of pro-apoA-I and increased HDL levels. *J Lipid Res*. 2011;52:1974–1983.
46. Dyrlund TF, Poulsen ET, Scavenius C, et al. Human cornea proteome: identification and quantitation of the proteins of the three main layers including epithelium, stroma, and endothelium. *J Proteome Res*. 2012;11:4231–4239.
47. Galiacy SD, Froment C, Mouton-Barbosa E, et al. Deeper in the human cornea proteome using nanoLC-Orbitrap MS/MS: an improvement for future studies on cornea homeostasis and pathophysiology. *J Proteomics*. 2011;75:81–92.
48. Karring H, Thogersen IB, Klintworth GK, Moller-Pedersen T, Enghild JJ. A dataset of human cornea proteins identified by Peptide mass fingerprinting and tandem mass spectrometry. *Mol Cell Proteomics*. 2005;4:1406–1408.

Investigative Ophthalmology & Visual Science